Bioelectrochemistry and Bioenergetics, 28 (1992) 319–340
A section of *J. Electroanal. Chem.*, and constituting Vol. 343 (1992)
Elsevier Sequoia S.A., Lausanne

JEC BB 01522

On the dielectric properties of cell suspensions at high volume fractions *

Chris L. Davey, Hazel M. Davey and Douglas B. Kell **

Department of Biological Sciences, University College of Wales, Aberystwyth, Dyfed SY23 3DA (UK)

(Received 24 November 1991)

Abstract

The dielectric increment $\Delta\epsilon'$ of the β-dispersion of biological cell suspensions is given (H.P. Schwan, Adv. Biol. Med. Phys., 5 (1957) 147) by the equation $\Delta\epsilon' = 9PrC_m/4\epsilon_0$, where cells of radius r and of a membrane capacitance C_m farads per unit area are suspended at a volume fraction P. This equation predicts that $\Delta\epsilon'$ is proportional to P at all values of P, a prediction which is not borne out at high values of P. To deal with this problem, it has been suggested (but never adequately checked) that a better fit is obtained from the equation $\Delta\epsilon' = (9rC_m/4\epsilon_0)P/[1+(P/2)]^2$, in which the term $1/[1+(P/2)]^2$ models the loss of linearity as the volume fraction increases. This term depends only on P and is independent of the cell radius r. By making careful and independent measurements of P, r and $\Delta\epsilon'$ for a number of bacterial and yeast cell suspensions, we show herein that this equation holds true over a wide range of volume fractions and cell sizes. Thus, the correction factor for the non-linear relationship between $\Delta\epsilon'$ and P is indeed independent of the cell radius. This has the important and useful consequence that a simple calibration curve of dielectric increment vs. dry weight or cell numbers permits one to determine the specific enclosed volume of the strain of interest, i.e. the volume enclosed by the cytoplasmic membranes of the cells per unit biomass. Finally, we show that the dielectric increment per unit biomass is directly proportional to the cell radius.

INTRODUCTION

The passive-electrical (dielectric) properties of biological materials are an area of intense interest. Indeed, as early as the end of the last century the study of the low frequency conductivity of blood not only indicated the possible presence of a poorly conducting layer around cells but also led to formulae (albeit empirical) that allowed the conductimetric assessment of haematocrit [1–4].

* This paper is dedicated to Professor G. Milazzo, on the occasion of his 80th birthday, in recognition of his enormous contribution to the development of bioelectrochemistry.

** To whom correspondence should be addressed.

With the development of theoretical models of the electrical properties of cells came more rigorous and incisive studies on cellular structure. By the 1920s Fricke's work [5] had achieved sufficient sophistication for him to be able to measure the membrane capacitance of erythrocyte membranes to be about 0.81 μF cm^{-2}. Using this value and an estimated value for the permittivity of the membrane constituents he calculated the membrane thickness to be some 3.3 nm. Both these values are close to those accepted today.

The power and utility of electrical measurements were thus apparent from a very early stage. However, the rigorous application of these methods to medical and other instrumentation has only become practical in recent times. The development of fully automated impedance analysers and powerful computers has enabled the measurement and analysis of electrical properties to be carried out with great speed and convenience. This, combined with the development of better models for the electrical properties of cells, and the substantial literature that has built up on them (for reviews see refs. 6–11), has enabled faster development of applications in this area.

A successful exploitation of the low-frequency electrical properties of cells for measurement purposes followed the development of the Coulter Counter [12–14]. This instrument relies on the very high impedance of cell membranes at low frequencies (much less than 100 kHz) which means that a cell suspension can be regarded (at such frequencies) as a suspension of non-conducting particles in a conducting suspension medium. The cells are forced to pass through a small orifice with electrodes on either side, with a constant amplitude d.c. current source between the electrodes. As a cell passes through the orifice it causes a transient voltage increase which yields quantitative information on the cell size. A correlation of such peaks with the amount of suspension drawn through the orifice gives the concentration of cells in the suspension.

Not surprisingly there is much interest in the development of medical diagnostic methods involving electrical properties [15–17]. These include impedance pneumography [18], plethysmography [19–22] and imaging (impedance tomography [23–27]). The use of conductimetry to measure haematocrit has also continued to be studied [28–30].

An area of study since the last century has been "impedance microbiology" [14,16,31,32]. Here one monitors the effect of the growth of microorganisms on the conductance of the medium in which they are grown. In some cases the parallel effects of this on the polarization of the measuring electrodes is also monitored by measuring the system's capacitance at the same low frequency. This has been commercialized and is used in the rapid identification and enumeration of cells in both food and medical microbiology. However, impedance microbiological methods constitute only an indirect method of measuring cell growth. Of more interest to us is the direct measurement of cell population growth by monitoring the dielectric (electrical) properties of the organisms themselves.

The dielectric properties of biological materials, in the frequency range below some 100 MHz, are measured by immersing a pair of electrodes in the cell

suspension of interest [33–35]. A sinusoidal current at a known frequency is then passed through the suspension and the resultant voltage and phase angle measured. From these one can then calculate the values for the equivalent parallel arrangement of idealized capacitor (C in farads) and conductor (G in siemens) which model the suspension's properties at each frequency (f in hertz) measured (i.e. one works in the admittance domain, see ref. 36). The values of capacitance and conductance measured depend on the geometry of the notionally parallel-plate electrodes used. Thus they must be normalized to values that are independent of the electrode arrangement before they can be conveniently related to mathematical models of the frequency-dependent electrical properties of the cell suspension. To this end one converts the capacitance values to relative permittivity (ϵ', which is dimensionless) and the conductance to conductivity (σ' in siemens per metre) using eqns. (1) and (2) respectively [8,37]:

$$\epsilon' = C(d/A\epsilon_0) \tag{1}$$

$$\sigma' = G(d/A) \tag{2}$$

The electrode geometry is thus characterized by the cell constant (d/A), where A is the area of one of the parallel plate measuring electrodes and d is the distance between them, the cell constant therefore having units of reciprocal metres. ϵ_0' is the permittivity of free space (vacuum) and is a constant of value $8.854.10^{-12}$ F m^{-1}. The relative permittivity ϵ' is dimensionless as it is the ratio of the absolute permittivity of the material between the electrodes (in farads per metre) and ϵ_0'. ϵ' reflects the ease and extent to which localized charge distributions in the material can be distorted by an applied electric field [8]. The conductivity σ' gives a measure of the ease with which delocalized electric charges can migrate through the medium under the influence of the field. In the biological systems discussed in this article, the charges are aqueous ions and so conductivity depends on the ion concentrations, their mobilities and valencies. As may be seen from eqn. (2) the conductivity is numerically equal to the conductance of an electrode of unit dimension.

The permittivity and conductivity of biological cells are markedly frequency dependent [7–9,38,39]. As the frequency increases the permittivity falls, and the conductivity increases, in a series of broad steps called dispersions. There are two major dispersion mechanisms of interest for cell suspensions in the frequency range below 100 MHz.

The lower frequency dispersion is known as the α-dispersion [6,7,37], and is typically centred around 1–10 kHz for cells. As cells are negatively charged they have around them a diffuse cloud of counter-ions which can migrate tangentially to the cell surface under the influence of an applied electric field, effectively setting up an induced dipole moment along the cell. As this ionic migration takes a finite time to occur, its extent will decrease as the frequency of the applied field increases, resulting in the cell dipole moment (and hence suspension permittivity) decreasing with increasing frequency [6–9,40–42]. Not all cells have a significant α-dispersion; typical of these are the yeasts [6,43–47] and cultured animal cells

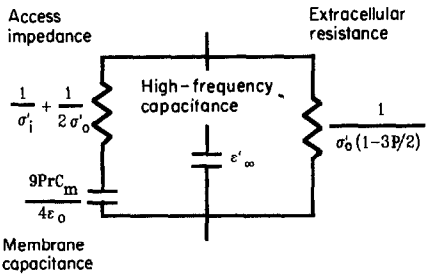

Fig. 1. Electrical equivalent circuit for describing the β-dispersion of biological cell suspensions, in which cells of radius r, internal conductivity σ_i and of a membrane capacitance C_m farads per unit area are suspended in a medium of external conductivity σ_0 at a volume fraction P. ϵ_0 is the permittivity of free space.

[6,48–51]. Those cells that have been found to have prominent α-dispersions are usually also known to have large surface charge densities; typical amongst these are red blood cells (under some preparation conditions, see refs. 6 and 52) and the Gram-positive bacteria [6,53].

The second major dispersion is the β-dispersion. This is typically centred at frequencies between 100 kHz and 10 MHz. This dispersion is mainly due to ionic charging of the plasma-membrane capacitance of the cells under the influence of the applied electric field [5–7,10,54–57]. This membrane charging is mediated via the conducting cell cytoplasm and suspension medium, both of which have finite conductivities (resistivities). Thus the suspension can be represented by a resistor–capacitor network [38] which has a time constant that reflects the time needed to charge up the plasma-membrane (Fig. 1). As the frequency is increased, the admittance of the plasma membrane increases and so a smaller potential is dropped across it. As this induced membrane potential falls so does the extent of charging of the membrane's capacitance. Thus the amount of charge stored by the suspension falls for a given applied voltage and so therefore must the suspension's capacitance (permittivity).

At low frequencies the plasma-membrane has a very low admittance (the membrane's intrinsic conductivity is so small that it is generally set equal to zero in the formulation of suspension models) and so most of the current must flow around the cells. Thus at these frequencies the cell suspension can be regarded as a suspension of non-conducting particles in a conducting medium (see the discussion of the Coulter counter above). Thus one can expect, and indeed finds, that there is a conductivity decrement relative to the suspending medium, that is roughly proportional to the volume fraction of cells present. Several equations have been proposed to model this effect [58–61], the most suitable for biological materials apparently being that of Bruggeman [58,62–64]:

$$R = \frac{\sigma'_1}{\sigma'_0} = (1 - P)^{2/3} \tag{3}$$

in which σ_l' is the low frequency conductivity of the cell suspension, σ_0' is the conductivity of the suspending medium and P is the volume fraction of cells present. It is clear from this equation that measurement of σ_l' and σ_0' provides a very convenient method of measuring volume fractions, and indeed has been used successfuly to do so [62–64].

At high frequencies the plasma-membrane admittance is very high and so the current can flow through the cells as well as around them. Thus the conductivity of the cell suspension increases, as the cytoplasmic conductivity is now seen by the field.

For this study we are mainly interested in measuring the effect of frequency on the permittivity of the cell suspension in the region of the β-dispersion, as this enables us not only to monitor the biomass content of a cell suspension (see refs. 65 and 66 and later) but also to calculate various cellular properties [6,38]. As the frequency is increased the permittivity falls from a high low-frequency plateau to a low high-frequency plateau according to the Cole–Cole equation [67,68]:

$$\epsilon_\omega' = \frac{\Delta\epsilon'\left[1 + (\omega\tau)^{1-\alpha}\sin(0.5\alpha\pi)\right]}{1 + 2(\omega\tau)^{1-\alpha}\sin(0.5\alpha\pi) + (\omega\tau)^{2-2\alpha}} + \epsilon_h' \tag{4}$$

where ϵ_ω' is the permittivity at the frequency of interest, ϵ_l' and ϵ_h' are the limiting permittivities at frequencies low and high relative to the mid-point of the β-dispersion. $\Delta\epsilon'$ is the dielectric increment of the β-dispersion (and equals $\epsilon_l' - \epsilon_h'$). τ is the relaxation time of the β-dispersion (in seconds) and is related to its critical frequency (f_c in hertz) by $f_c = 1/(2\pi\tau)$. f_c is the frequency at which the permittivity has fallen to $(\Delta\epsilon'/2) + \epsilon_h'$. α is the Cole–Cole α value and is thought to reflect the magnitude of the distribution of relaxation times underlying the dispersion (see refs. 10 and 69).

$\Delta\epsilon'$ and τ for the β-dispersion can be related to the structure of the cell suspension (if say $P < 0.2$) by the equation [10]

$$\Delta\epsilon' = \frac{9PrC_m}{4\epsilon_0} \tag{5}$$

$$\tau = rC_m\left[\frac{1}{\sigma_i} + \frac{1}{2\sigma_0}\right] \tag{6}$$

Here r is the cell radius (in metres), C_m is the membrane capacitance per unit area (in farads per square metre), σ_i' is the cytoplasmic conductivity (siemens per metre) and the other terms have the same meanings as described above.

Our interest in eqn. (5) is two-fold. First, if one measures $\Delta\epsilon'$, r and P it is possible to calculate the membrane capacitance C_m. Secondly, for purposes of instrumentation, the fact that $\Delta\epsilon'$ is directly proportional to the cellular volume fraction P, provided that r and C_m remain approximately constant as they seem to

do for most fermentations, means that one can monitor cell population growth in real-time by measuring $\Delta\epsilon'$. Ideally one would do a frequency scan of the permittivity of the cell suspension, and fit eqn. (4) to the data by non-linear least-squares methods [33,70–74] to obtain the true $\Delta\epsilon'$ value. In reality what is usually done is that one backs off the permittivity of the growth medium to zero prior to inoculating the culture [65]. This in effect sets ϵ'_h to zero as this is largely due to the water content of the growth medium and is only rather weakly dependent on P and changes in salt concentration [9]. One then picks a frequency well into the low-frequency plateau region of the β-dispersion and as the cell population increases the permittivity recorded at that frequency is approximately equal to $\Delta\epsilon'$ and hence to the cellular concentration.

To enable the use of dielectric measurements in a fermentation environment we have developed a dielectric spectrometer (now called the Biomass Monitor) that operates at frequencies between 0.2 and 10 MHz. The machine uses four-terminal electrodes to reduce electrode polarization effects [35,67,75], and has an electrolytic cleaning mechanism to allow cleaning of the electrodes in situ [76]. The machine as used in this study has been constructed to allow either frequency scanning or operation at one frequency. We and others have shown in previous publications the utility of the dielectric method for the measurement of biomass of a variety of biological systems [77]. These include bacterial and yeast cultures [55,65,66,69,78,79,80], bacterial biofilms [76], plant and animal cell cultures [49,64,81], immobilized cells [82] and filamentous fungi growing on solid substrates [83,84].

$\Delta\epsilon'$ is linear with the cellular biomass to very high concentrations. However, at volume fractions greater than say 20% a deviation from linearity is clearly seen (for examples see the data in refs. 45, 46 and 85–88). Instead of a linear increase in permittivity with biomass concentration, as predicted by eqn. (5), one finds that the curve tends to a plateau. In the majority of fermentation processes such high biomasses are never achieved. However, this is not the case for many fed-batch systems where biomass concentrations well into the non-linear region can be found. The application of the dielectric method to control of the pitching of highly concentrated yeast slurries in the brewing industry also demands that the permittivity (capacitance) be linearized [78]. Further examples where linearization of the signal is desirable include the study of blood dielectric properties for diagnostic purposes (here volume fractions are typically 45%) and for control of the biomass content on cell slurries prior to centrifugation, where the efficiency of the centrifugation depends on the cell concentration. Also it is important when using eqn. (5) in the calculation of C_m that the measured $\Delta\epsilon'$ is still in the linear region, or erroneously small C_m values will result [6].

This loss of linearity between $\Delta\epsilon'$ and P at high volume fractions is a result of the cells distorting the electric field which impinges on the cells around them. The suspension eqns. (5) and (6) were derived on the basis that the cell suspensions were sufficiently dilute that this did not occur. The extension of the low-P equations to higher volume fractions is far from simple [38] but several attempts

have been made [89–91]. Perhaps the potentially most useful from a practical viewpoint is the equation published by Schwan [45,90,91]:

$$\Delta\epsilon' = \frac{9rC_m}{4\epsilon_0} \frac{P}{[1+(P/2)]^2} \tag{7}$$

The effect of the right-hand term in eqn. (7) is to cause a monotonic decrease in the otherwise linear relationship between $\Delta\epsilon'$ and P, such that at $P = 0.2$, $\Delta\epsilon'$ is 17.4% lower and at $P = 0.4$ $\Delta\epsilon'$ is 30.6% lower than it would be if eqn. (5) held.

In principle τ might also be expected to vary with P, owing to the behaviour encapsulated in eqn. (7). Indeed, appropriate equations have been formulated. However, the predicted P-dependence of τ is rather weak, and would be difficult to establish experimentally owing to the changes in cytoplasmic and suspension medium conductivity as a function of time caused by leakage of ions from the cells or by metabolic activity.

Equation (7) is merely eqn. (5) modified by a term $1/[1+(P/2)]^2$ that models the loss of linearity as the volume fraction increases. However, we are not aware of any detailed attempts to test the concordance of this equation with experimental reality. It is particularly noteworthy that this term depends only on P and is independent of the cell radius r. The chief aim of the present work was therefore to test eqn. (7) over a very wide range of known volume fractions, from dilute suspensions to cell pastes, and to do this over a range of cell sizes. It was found that the data could in all cases be well fitted to eqn. (7), showing that the correction factor for the non-linear relationship between $\Delta\epsilon'$ and P is indeed independent of the cell radius, and thus may in principle be used for all types of cell suspension.

MATERIALS AND METHODS

Organisms used

Three industrial strains of the yeast *Saccharomyces cerevisiae* were used. Two of the strains were obtained as cell pastes; these were Distillers Company Limited (DCL) "High Activity Baker's Yeast" and DCL "Distillery Yeast". The cells in these pastes had bud counts of 13% and 2% respectively and so were deemed to be in stationary phase. The third yeast (BB 11) was obtained as a pure isolate from the brewing industry. BB 11 was grown to a high biomass in a batch fermentation in a medium consisting of 1.3% E-broth and 5% malt extract (both from Lab M) at a starting pH of 6.0. The non-baffled fermentor had a working volume of 5 l, the medium was not sparged with air and was only stirred gently (75 rev min^{-1}) to keep most of the contents in suspension. The pH was not controlled but the temperature was held at 30°C throughout the 22 h growth period. After this growth period the cells had reached stationary phase (5% budding) and were harvested by centrifuging the cells to a pellet.

In addition the bacterium *Micrococcus luteus* (formerly called *Micrococcus lysodeikticus*) Fleming strain 2665 was used. This was grown in batch culture in 5 l

of E-broth (pH 7.4). The medium was gently sparged with air and the stirrer speed was set to 270 rev min^{-1} (with baffles present) as this gave a reasonable gas hold-up without too violent aeration which from previous experiments was found to inhibit growth. The temperature and pH were controlled at 30°C and 7.4 respectively and the foam was regulated with Sigma-B silicone anti-foam. After 34 h growth the fermentor contents were harvested as described for the BB 11 yeast above.

These organisms were chosen because they are approximately spherical. This fact meant that one could apply eqns. (3), (5), (6) and (7) to the data with confidence, as they were all derived for spherical objects. As the yeast cells used were all in stationary phase the percentage of cells budding was fairly low, as judged by scoring 100 cells from the washed pellet. This meant that uncertainty in the cell counts and sizes due to the fact that it is very difficult to judge whether an attached bud still has cytoplasmic continuity with its mother cell was much reduced. In all the cell counts, measurements and calculations, the attached buds were ignored.

Preparation of the cells

All the cells were washed and resuspended in the same suspension buffer (SB). This contained (in millimolar) KH_2PO_4 50, $MgSO_4 \cdot 7H_2O$ 5, adjusted to pH 7.0 with 5 M KOH. SB was made up fresh for each experiment, all reagents were from BDH, and the water was singly distilled in an all glass apparatus.

The pellet of cells either harvested from batch culture or cut from a block of paste, was suspended in at least three times its volume of suspension buffer (SB). The resulting suspension was centrifuged at 1000 *g* (yeast) or 2750 *g* (*M. luteus*) for 10 min at room temperature. The supernatant and any precipitated growth medium components from the top of the pellet were discarded and the cells resuspended in fresh SB. These were then left at room temperature for 45 min, with occasional mixing, to allow the cells to equilibrate with the medium and to allow any limited growth triggered by the resuspension of the cells to occur. The cells were recentrifuged as described above and the supernatant was discarded. A final wash was done in suspension buffer followed by another centrifugation to obtain a pellet. The pellet was normally left slightly inclined for a while to allow any excess buffer to run off. In addition in the case of *Micrococcus* it was found that the pellet obtained after the washing procedure still contained a lot of buffer. Therefore, to perform the very high volume fraction measurements, a sample of the pellet was further centrifuged at 13 000 rev min^{-1} in a bench Eppendorf-type centrifuge for 30 min and any supernatant removed.

Dielectric measurements

All the cell suspensions were analysed using a Biomass Monitor (BM, formerly called a Bugmeter, Aber Instruments Ltd, Science Park, Aberystwyth SY23 3AH). The machine was switched on at least 30 min prior to use. The electrode used was

of the "Mexican Hat" type [92], and consisted of an epoxy resin body with a 1 ml cavity in it, which contained four solid, 24-carat gold electrode pins. The electrode was thoroughly washed prior to each experimental series with water then detergent then water followed by neat ethanol then distilled water and finally by applying the electrolytic cleaning pulses to the electrode whilst it contained dilute aqueous KCl. After the electrolytic cleaning the electrodes were left for at least 30 min prior to use. The electrode was never allowed to dry out during the experiments and was well rinsed with distilled water between each cell sample. The cell constant of the electrode was calculated from eqn. (2) using the measured conductance of 10 mM KCl (at 0.48 MHz) at a known temperature (i.e. known conductivity). The sensitivity of the instrument is switchable, and this is taken into account when measuring the cell constants. Typical values were 0.9 cm^{-1} for the *Micrococcus* and 1.8 cm^{-1} for the yeast experiments. The electrode was always filled to the same volume (1 ml) during the experiment to prevent error due to any depth-dependency of the cell constant.

Each cell suspension was scanned at ten frequencies between 0.2 and 10 MHz, which were chosen to give an even spacing on a log frequency (hertz) scale. The order in which these frequencies would be used in the scans was chosen at random. For the two DCL yeasts the frequency scans were carried out by manually adjusting the frequencies and noting the capacitance and conductance values. A 1 s low pass filter was used to remove any noise on the signal and so the readings were taken once the signal had stabilized at its new value. In these cases the Biomass Monitor (BM) capacitance at 0.4 MHz was zeroed in the suspension buffer prior to the experiment. For the remaining two organisms the scans were carried out under full computer control using a program called "MINISCAN", written in-house in Microsoft Quick BASIC 4.5. This time the BM was left in absolute capacitance mode and ten replicate readings at 0.1 s intervals were taken at each frequency and averaged. The capacitance and conductance data were converted to their equivalent permittivities and conductivities using eqns. (1) and (2); in the case of the manual scans this was done on a spreadsheet (VP-Planner) template [93] whilst the data scanned by computer were converted as they were recorded.

For each cell suspension scanned a polarization control was done as described in refs. 55 and 67. This entailed adjusting a 1 ml sample of the suspension medium to the same conductance (at 0.2 MHz) as the cell suspension of interest. This was then scanned as for the cell suspensions. The polarization controls were then subtracted from their equivalent cell data to give the final dielectric data. This subtraction process was carried out in software for the data scanned by MINISCAN or in the same spreadsheet template mentioned above for the manually acquired data. (This set ϵ_h to a value of approximately 0; since our concern here was with the values of $\Delta\epsilon'$, we did not seek to add back the appropriate value of ϵ_h.)

A single Cole–Cole equation for permittivity (eqn. (4)) was fitted to each set of finalized dielectric data. This was done using the program GraFit 2.0 (Erithacus

Software Ltd., PO Box 35, Staines, UK). The dielectric data were passed to the program either by making an ASCII file (.prn) from the spreadsheet template or directly using the data files created by MINISCAN and its subsidiary programs. GraFit used the non-linear least-squares method of Levenberg and Marquardt [33,70,72,94] to find the optimum fit. In all cases "simple" weighting was used, together with the "robust" weighting algorithm of Mosteller and Tukey [95] (see also ref. 96).

Cell size measurements

The size and axial ratio distributions of each cell type were determined from photomicrographs. Light microscopy was used as it avoids all need for special fixation procedures and dehydration processes needed for electron microscopic work, which will affect the cell sizes. A Polyvar microscope incorporating a 35 mm camera was used for all the microscopy work. The yeasts were photographed under conventional optics while Normaski optics were used for the rather smaller micrococci. Photographs were taken under oil-immersion at a total magnification of 1250 ×. Photographs of 10 μm diameter latex beads (Dyno Particles A.S, PO Box 160, Lillestrøm, Norway) taken under the same conditions as for the cells were used for calibration purposes.

The photographs were developed and printed at a magnification of 3.5 × except for the photographs of the *Micrococcus* (and the corresponding set of latex beads) which were magnified 10 ×. The resulting photographs for each organism were mixed up randomly with photographs for the same cell type but done under slightly different conditions for other (flow cytometric) experiments to be described elsewhere. The pictures were identified only by a code number, the meaning of which was not known to the person measuring the cells, such that the measurements were done blind. The photographs were placed in turn under an approximately 1.5 × bench magnifying glass and the long and short axes of the cells were measured with vernier callipers; measurements were made to the nearest 0.1 mm (after magnification had been taken into account this corresponded to about 0.1 μm). All the photographs for the cell types were analysed by the same person using the same callipers to keep systematic errors constant. Every cell (apart from unseparated buds) of the yeasts that were in focus were measured, but in the case of the photographs of *M. luteus*, all the in-focus cells from a randomly selected quarter of the photograph were used. Between 110 and 190 cells were measured for each cell type.

The dimensions of the cells (recorded in millimeters from the photographs) were entered onto a spreadsheet and converted to their true size by using a calibration based on the mode size of a sample of 10 μm beads which had been described as above. The corrected lengths of the long and short axes of the cells were then used to calculate the volume of the equivalent ellipsoid of revolution and the radius of the sphere of equal volume to the ellipsoid.

The volume of an ellipsoid of revolution [33] is given by the equation:

$$V_e = \tfrac{4}{3}\pi ab^2 \tag{8}$$

where V_e is the volume, a is the long semi-axis and b is the short semi-axis of the ellipsoid. From this we can derive eqn. (9) which gives the equivalent radius for a sphere with the same volume of the ellipsoid:

$$r_s = \left[\left(\frac{L}{2}\right)\left(\frac{S}{2}\right)^2\right]^{(1/3)} \tag{9}$$

where r_s is the radius of the equivalent sphere, L is the length of the measured long axis and S is the length of the measured short axis of the cell.

Dry weights

For each cell type a series of dilutions in SB of the prepared cell pellet was made and each was scanned as above. In the case of the "solid" samples the paste was carefully pressed into the 1 ml electrode cavity taking care not to bend the electrode pins. As these solid samples were not easily amenable to volume fraction measurements the dry weight of all the suspensions scanned were measured. Volume fraction measurements were only done on the suspensions at higher dilutions and so a calibration curve of these measurements vs. their equivalent dry weights could be used to estimate the volume fractions of the more concentrated suspensions.

For the solid suspensions the contents of the electrode cavity (1 ml) were washed into a known volume of SB prior to dry weight measurements. For the more dilute suspensions the electrode contents were diluted in SB prior to dry weight analysis. A preweighted 25 mm diameter 0.2 μm pore size Whatman filter (WCN type, cellulose nitrate, plain white) was wetted with distilled water and placed under gentle vacuum. A sample of the diluted cell suspension (typically 1 ml) was then placed on the filter and sucked "dry". The cell pellet was then washed with 0.5–1 ml of distilled water and again sucked "dry". The filter was then reweighed to give the wet weight of cells per millilitre. After drying the filter overnight at 100°C the dry weight per millilitre could be determined.

Volume fraction measurements

For the more dilute suspensions of each cell type, volume fraction measurements were performed. For the yeast, volume fractions were calculated from conductivity measurements using eqn. (3) as well as from calculations based on cell numbers per millilitre (from haemocytometer counts) and the mean volumes of the ellipsoids of revolution (from eqn. (8)) corresponding to each cell type measured on the photographs. For the micrococci only the conductivity method was used as

the haemocytometer counts proved to be unreliable for such small cells under the conditions used.

The same haemocytometer (Weber Scientific International Ltd, Improved Neubauer type, depth 0.1 mm) was used throughout the study by the same person to keep systematic errors constant. To ensure consistent and reliable results from the counts the following procedure was used throughout. The chamber was loaded once for each dilution and all 400 small squares (each $1/400$ mm^2) were counted. The suspensions were diluted such that this total count gave between 540 and 2200 cells [97]. Attached buds were not counted. The counting was done under normal optics at a total magnification of $100\times$ on a microscope.

The conductivity measurements of the volume fraction of cells were performed using an EDT RE 387 Series 3 microprocessor conductivity meter. The electrode cell had two platinum-blacked electrodes. Under the conditions used here the operating frequency was 300 Hz and the excitation voltage 150 mV. The electrode had been modified to work with a volume of 1.5 ml and this was used throughout. The cell constant of this arrangement as calculated for the BM above was 1.1 cm^{-1}. All measurements were performed with the machine's temperature compensation feature deactivated owing to the unknown temperature coefficients of the samples used. A sample of the cell suspension was first measured (σ_1' in eqn. (3)) and then it was immediately centrifuged for 5 min at 13000 rev min^{-1} in an Eppendorf-type bench centrifuge, and the resulting supernatant was then measured (σ_0' in eqn. (3)). The volume fraction P was then calculated from eqn. (3).

RESULTS AND DISCUSSION

Figure 2 shows the distributions of axial ratios for the four organisms used, as measured from the photomicrographs. It is evident that the great majority of the cells are very nearly spherical. Thus one can safely use the radius of the sphere of equivalent volume in dielectric calculations [43]. Figure 3 shows the distribution in cell sizes for each cell type based on this approach. The organisms chosen are of different sizes except for the two DCL yeast strains which are close together. Each strain also shows a fairly wide distribution in cell sizes, a fact that seems to hold true for many organisms [98].

Figure 4 compares the volume fractions P determined in two different ways for the three yeast strains. The P values derived from the conductivity measurements P_σ were calculated from eqn. (3), as described in the methods section. The other P values P_H were calculated from the haemocytometer measurements and the mean volume of the ellipsoids of revolution corresponding to each cell type. As may be seen (Fig. 4), the two ways of calculating volume fraction give very similar results. However, of the two, the systematic errors in the haemocytometer counts are likely to be the more significant [49,97,99–101]. Workers using conductimetry to measure haematocrit, using methods and equations very similar to those we have used to measure P, have also encountered this problem. Several careful pieces of work (e.g. refs. 30 and 102) have shown that the errors in the haemocytometer measure-

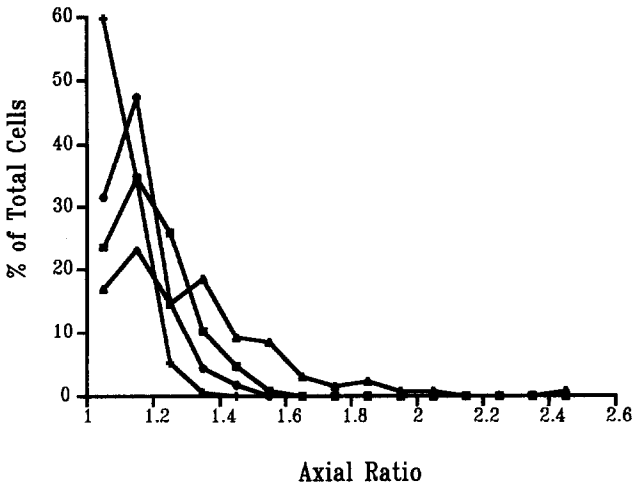

Fig. 2. Histogram illustrating the distribution in axial ratios of the strains used herein. Cells were examined photomicrographically as described in the Materials and Methods section. Each bin of the histogram represents cells falling in the range $n \pm 0.1$, where n is the mid-point axial ratio plotted: ■ distiller's yeast, + baker's yeast, ◆ BB 11 yeast, ▲ *Micrococcus luteus*. The mean values of axial ratio were respectively, 1.18, 1.09, 1.15 and 1.31.

ments are large compared with those from conductimetry. A further point is that the conductivity-based measurement of volume fraction measures only the protoplast inside the cell wall. The estimates of P relying on the measurements of the cell numbers (i.e. P_H) also include the cell wall in the cell volumes. This may in part explain why the slopes of the fitted lines on Fig. 4 are all slightly less than unity. We therefore used the volume fractions from the conductimetry as our P values for the dielectric calculations. Table 1 contains the values for the haemocytometer counts along with the other parameters measured for each cell type.

Figure 5 shows the permittivity data as a function of frequency for two of the organisms used. The very good fits to the data using the Cole–Cole equation shown in Fig. 5(A) were typical of the data for all three yeast strains at all the dilutions tested. The *Micrococcus* data, however, were more problematic (Fig. 5(B)). Not only was the f_c of the β-dispersion too high to allow the data to be fitted to the Cole–Cole equation from the data obtained with the available frequency range [33], but a substantial α-dispersion was also present. This low-frequency effect could be ascribed to an α-dispersion rather than to electrode polarization because (i) the data were already corrected for electrode polarization via subtraction (see Materials and Methods and ref. 67), and (ii) the magnitude of the effect increased with the cellular concentration. As micrococci are Gram-positive, the presence of an α-dispersion is not wholly unexpected. The effect of the polarization controls was to set ϵ'_h close to zero so one could estimate the magnitude of $\Delta\epsilon'$ from the permittivity at a single frequency that was higher than

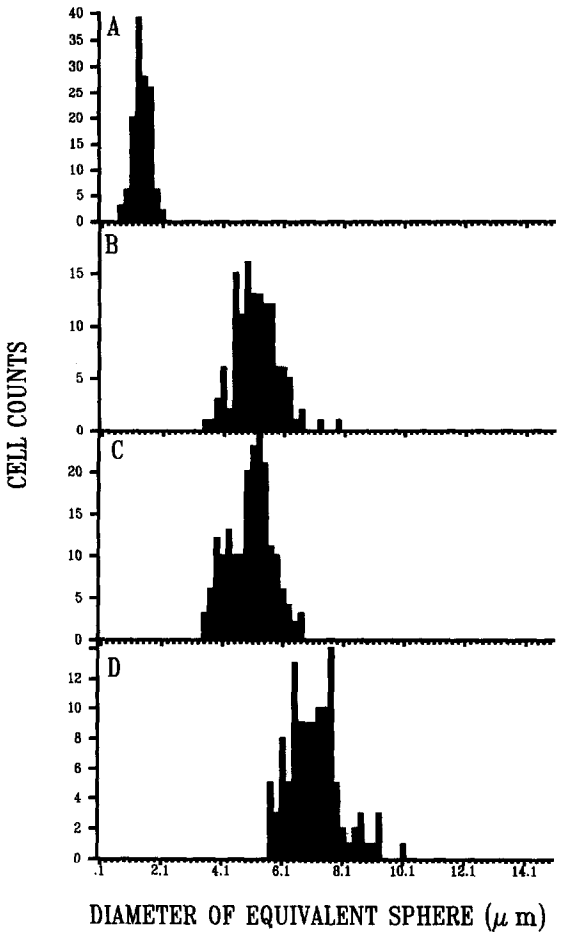

Fig. 3. Histogram illustrating the distributions in cell sizes of the strains used herein. Cells were examined photomicrographically as described in the Materials and Methods section, and their volumes converted to those of spheres of the equivalent radius. Each bin of the histogram represents a band of 0.2 μm: (A) *Micrococcus luteus*, (B) distiller's yeast, (C) baker's yeast, (D) BB 11 yeast. The mean values of the cell diameters were respectively, 1.4, 5.2, 5.0 and 7.2 μm.

those seriously influenced by the α-dispersion but still on the low-frequency plateau of the β-dispersion. The frequency chosen for this was 2.71 MHz.

Figure 6 shows the relationship $\Delta\epsilon'$ and the volume fraction (as determined conductimetrically) for each cell type. Plotted on each graph are the best fits to the data for eqns. (5) and (7). In the former case the slope of the fitted straight line is the $9rC_m/4\epsilon_0$ term in eqn. (5). Since the values of $\Delta\epsilon'$ and P in eqn. (7) were known the fitting of this was also carried out by iterating the value of $9rC_m/4\epsilon_0$ until the optimum fit was achieved. Also shown on each of the graphs is a plot of

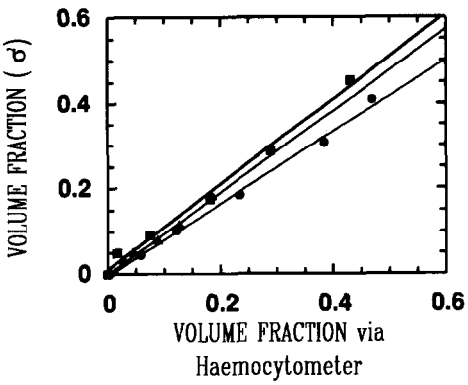

Fig. 4. Relationship between volume fractions estimated conductimetrically and microscopically. Measurements were performed as described in the Materials and Methods section and in the text. The lines represent the best fits to the data: ● baker's yeast, ■ distiller's yeast, ▲ BB 11 yeast.

eqn. (5) using the $9rC_m/4\epsilon_0$ term calculated from eqn. (7) inserted into it. When this is done eqn. (5) becomes

$$\Delta\epsilon'_{lin} = \frac{9rC_m}{4\epsilon_0} P_\sigma \tag{10}$$

where $\Delta\epsilon'_{lin}$ is the linearized value of $\Delta\epsilon'$. In all cases the better fit to the data is obtained from eqn. (7); this point is illustrated in Table 2. Even allowing for the weighting of Chi due to the robust weighting on each data point (see above), the fit achieved using equation (7) is far better than the linear fit using equation (5) in all cases.

Figure 7 illustrates an alternative way of fitting eqn. (7) to the data. For this one uses the measured dry weighting in milligrams per millilitre C instead of P_σ. The

TABLE 1

Relationship between dry weight, cell number and specific volume fraction for the strains used in the present work

Cell type	Wet weight: dry weight ratio	Cells per milligram of dry weight	P_σ/dry wt (ml mg^{-1})
Micrococcus	ND	ND	0.0021
Baker's yeast	4.63	$4.8(2)\times10^7$	0.0027
Distillery yeast	4.30	$3.4(1)\times10^7$	0.0027
BB 11 yeast	4.60	$1.2(5)\times10^7$	0.0024

Measurements were made as described in the Materials and Methods section and in the text. Volume fractions were measured conductimetrically, whilst cell numbers were obtained from haemocytometer counts. ND not determined owing to technical difficulties.

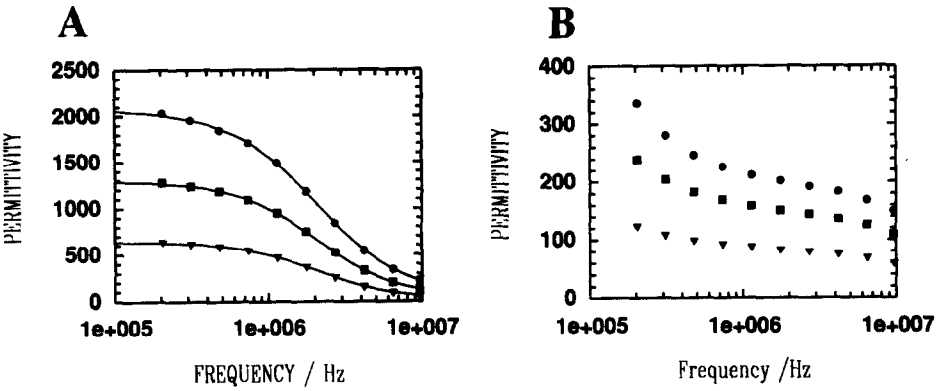

Fig. 5. Frequency dependence of the permittivity of typical cell suspensions studied. Measurements were performed as described in the Materials and Methods section and in the text: (A) yeast BB 11 at concentrations of ▼ 47, ■ 114 and ● 192 mg dry weight per millilitre, the lines represent the best non-linear least-squares fits of the data to the Cole–Cole equation; (B) *Micrococcus luteus* at concentrations of ▼ 49, ■ 94 and ● 143 mg dry weight per millilitre, the low-frequency data are dominated by an α-dispersion.

volume fraction terms in eqn. (7) are then replaced by CV_{sp}, where V_{sp} is the specific enclosed volume of the cells in millilitres per milligram dry weight [45]:

$$\Delta\epsilon' = \frac{9rC_m}{4\epsilon_0} \frac{CV_{sp}}{\left[1 + (CV_{sp}/2)\right]^2} \tag{11}$$

In this case, $\Delta\epsilon'$ and C are known from measurement, and thus the fitting is achieved by iterating two terms, namely V_{sp} and $9rC_m/4\epsilon_0$. Fits of as good a quality as Fig. 7 were achieved for each of the cell types used, again indicating the validity of eqn. (7).

Table 3 shows the values of the $9rC_m/4\epsilon_0$ term obtained from fitting eqns. (5), (7) and (11) to measured data of the type shown in Figs. 6 and 7. The fact that one can achieve good results using dry weights, without the need to measure P directly, is extremely useful when using the Biomass Monitor to obtain biomass values in fermentations with high cell concentrations. Usually when working with a new organism one draws up a calibration curve of $\Delta\epsilon'$ vs. cell dry weight (in milligrams per millilitre). Since we have shown that this curve will follow eqn. (11) we can fit that equation to the data and in the process gain a conversion factor V_{sp} that enables one to calculate volume fractions from the dry weight values alone. In other words, one can use eqn. (11) accurately to linearize the calibration curve. Additionally, V_{sp} is required in numerous bioenergetic and metabolic experiments, to obtain intracellular concentrations from measured amounts; the present method is much more convenient than, and gives comparable results with, those (usually based on isotope dilution experiments [103]) that are currently used.

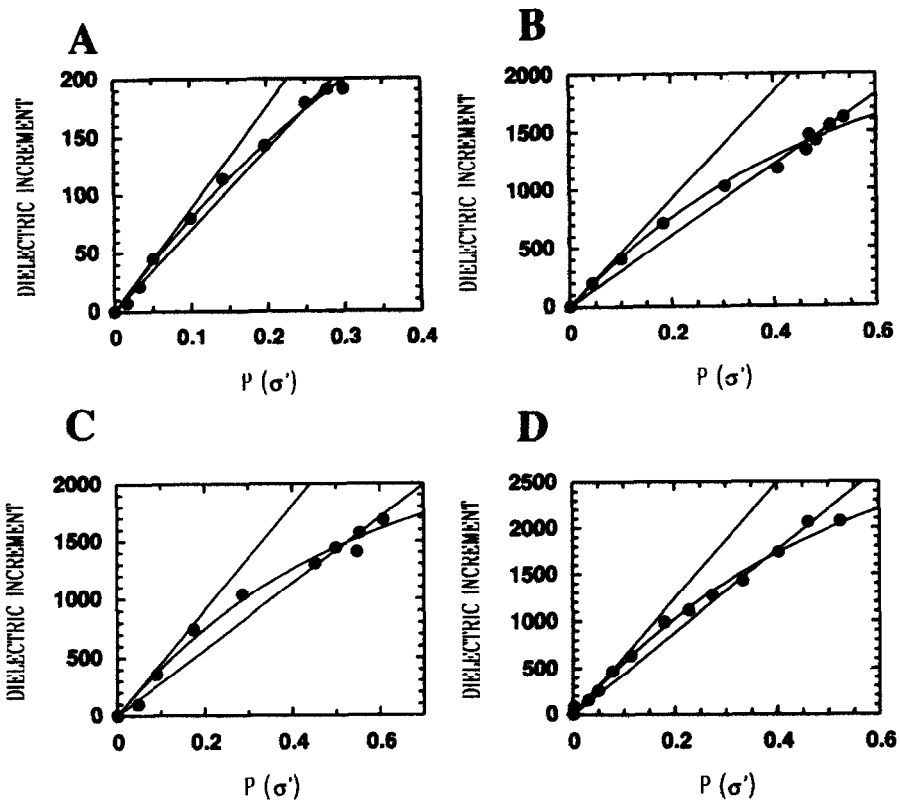

Fig. 6. Relationship between the dielectric increment and the volume fraction of cells. Dielectric measurements were carried out as described in the legend to Fig. 5, whilst measurements of P were performed conductimetrically as described in the Materials and Methods section and in the text. The lines constitute the best fit to eqns. (5), (7) and (10) as described in detail in the text: (A) *Micrococcus luteus*, (B) baker's yeast, (C) distillery yeast, (D) yeast BB 11.

Equation (5) predicts that the specific dielectric increment, i.e. the dielectric increment per unit biomass, should scale linearly with the (average) cell radius. The relevant $\Delta\epsilon'$ was obtained by fitting eqn. (7) to the measured $\Delta\epsilon'$ vs. P_σ data

TABLE 2

Statistical analysis of the volume fraction-dependence of the dielectric increments of the β-dispersion of the strains studied, the non-linear term in equation 7 clearly leads to a much better fit to the data

Cell type	Reduced chi^2 for the fit to eqn. (5)	Reduced chi^2 for the fit to eqn. (7)	Data from figure
Micrococcus	75	22	6(A)
Baker's yeast	4806	2441	6(B)
Distillery yeast	11140	4042	6(C)
BB 11 yeast	9981	2442	6(D)

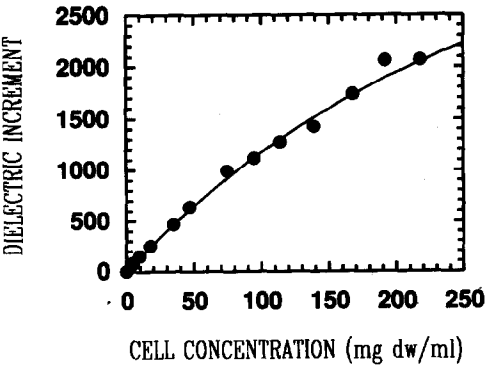

Fig. 7. Relationship between dielectric increment and cell concentration for yeast BB 11. Dielectric measurements were carried out as described in the legend to Fig. 5. The line constitutes the best non-linear least-squares fit to eqn. (11).

TABLE 3

Derived parameters for the organisms used in the present work

Cell type	$9rC_m/4\epsilon_0$ from eqn. (5)	$9rC_m/4\epsilon_0$ from eqn. (7)	$9rC_m/4\epsilon_0$ from eqn. (11)	V_{sp} (ml mg^{-1}) from eqn. (11)	V_{sp} (ml mg^{-1}) from Table 1
Micrococcus	698	881	842	0.0022	0.0021
Baker's yeast	3035	4609	5432	0.0021	0.0027
Distillery yeast	2840	4522	3907	0.0035	0.0027
BB 11 yeast	4402	6220	6620	0.0022	0.0024

Measurements were made as described in the Materials and Methods section and in the text. It may be observed (i) that eqns. (7) and (11) are highly self consistent, and (ii) that estimates of V_{sp} obtained conductimetrically are generally in excellent agreement with those obtained from permittivity measurements.

TABLE 4

Specific membrane capacitance and internal conductivity of the strains studied

Cell type	Membrane capacitance C_m (μF cm^{-2})	Internal conductivity σ_i (mS cm^{-1})
Micrococcus	0.49	ND
Baker's yeast	0.72	4.9
Distillery yeast	0.69	3.7
BB 11 yeast	0.68	4.0

Measurements were made as described in the Materials and Methods section and in the text, and the data from a number of dilutions fitted to eqns. (7) and (6) respectively. It was not possible to obtain σ_i for the *Micrococcus* data since f_c was too great for our measuring apparatus to obtain accurate data. C_m was calculated from the $9rC/4\epsilon_0$ term that was fitted according to eqn. (7), whilst σ_i was obtained from the measured relaxation time, mean radius and external conductivity according to eqn. (6).

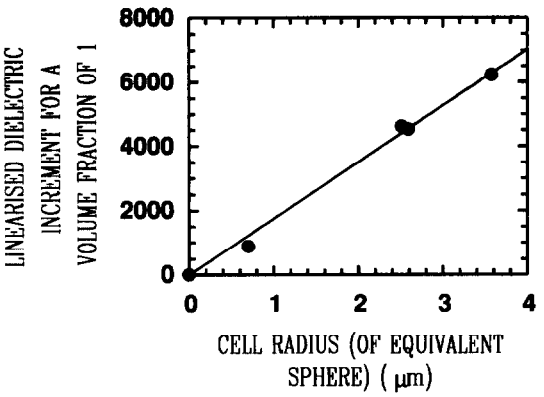

Fig. 8. Relationship between specific dielectric and cell radius. Dielectric measurements were carried out as described in the legend to Fig. 5, whilst measurements of the cell radii were performed as described in the legend to Figs. 2 and 3. The line constitutes the best linear least-squares fit to the data.

shown in Fig. (6). Figure 8 is a plot of the "linearized" $\Delta\epsilon'$ divided by the measured P_σ vs. the mean radius of the spheres of equivalent volume for each cell type. Whilst other mechanisms of dielectric relaxation probably contribute to the β-dispersion, they plausibly also scale with the cell radius [9,53,104]. Thus it remains true that the dielectric increment per unit biomass is indeed proportional to the (average) cell radius [6].

Finally, having measured P, r and $\Delta\epsilon'$ for the various cell types, it was possible to calculate C_m and σ_i (on the basis of the mean values of r), using eqns. (7) and (6) respectively. The relevant values of C_m and σ_i are tabulated in Table 4. It may be observed that the values of C_m are well within the range normally encountered [6,9,105] and (as with σ_i) rather independent of the strain of yeast used.

ACKNOWLEDGEMENTS

We thank the Science and Engineering Research Council, UK, Aber Instruments Ltd and FT Applikon Ltd for support of this work under the terms of the LINK scheme. We are also grateful to Drs. Neil Dixon, Arseny Kaprelyants and Bill Marsden for kindly providing the strains used.

REFERENCES

1 G.N. Stewart, J. Physiol., 24 (1899) 356.
2 G.N. Stewart, Am. J. Physiol., 90 (1929) 194.
3 G.N. Stewart, J. Boston Soc. Med. Sci., June 15 (16) (1897) 18.
4 G.N. Stewart, Zentralbl. Physiol., XI (1987) 332.
5 H. Fricke, J. Gen. Physiol., 9 (1925) 137.
6 C.L. Davey and D.B. Kell, The low-frequency dielectric properties of biological cells, in H. Berg (Ed.), Treatise on Bioelectrochemistry, Vol. VI, Birkäuser, Zürich, 1992, in the press.

7 K.R. Foster and H.P. Schwan, CRC Crit. Rev. Biomed. Eng., 17 (1989) 25.
8 R. Pethig, Dielectric and Electronic Properties of Biological Materials, Wiley, Chichester, 1979.
9 R. Pethig and D.B. Kell, Phys. Med. Biol., 32 (1987) 933.
10 H.P. Schwan, Adv. Biol. Med. Phys., 5 (1957) 147.
11 S. Takashima, Electrical Properties of Biopolymers and Membranes, Adam Hilger, Bristol, 1989.
12 Coulter Counter Industrial Bibliography, Coulter Electronics Limited, Luton, 1989.
13 Coulter Counter Medical and Biological Bibliography, Coulter Electronics Limited, Luton, 1989.
14 C.M. Harris and D.B. Kell, Biosensors, 1 (1985) 17.
15 C.L. Davey and D.B. Kell, in M. O'Connor, R.H.C. Bentall and J. Monahan (Eds.), Emerging Electromagnetic Medicine, Springer, Berlin, 1990, pp. 19–43.
16 D.B. Kell and C.L. Davey, in A.E.G. Cass (Ed.), Biosensors: A Practical Approach, Oxford University Press, Oxford, 1990, pp. 125–154.
17 M.F. Iskander and C.H. Durney, Proc. IEEE, 68 (1980) 126.
18 R.P. Henderson and J.G. Webster, IEEE Trans. Biomed. Eng., 25 (1978) 250.
19 L.E. Baker, in P. Rolfe (Ed.), Non-invasive Physiological Measurements, Academic Press, London, 1979:
20 F.A. Anderson, Ann. Biomed. Eng., 12 (1984) 79.
21 D.W. Hill, in P. Rolfe (Ed.), Non-invasive Physiological Measurements, Academic Press, London, 1979.
22 H.B. Wheeler and B.C. Penney, in V. Bernstein (Ed.), Non-invasive Diagnostic Techniques in Vascular Disease, Mosby, St. Louis, MO, 1982, pp. 104–116.
23 Anon, Clin. Phys. Physiol. Meas., 8 (Suppl. A) (1987) 181.
24 D.C. Barber and B.H. Brown, J. Phys. E, 17 (1984) 1.
25 T. Murai and Y. Kagawa, IEEE Trans. Biomed. Eng., 32 (1985) 177.
26 J.C. Newell, D.G. Gisser and D. Isaacson, IEEE Trans. Biomed. Eng, 35 (1988) 828.
27 L.R. Pryce, IEEE Trans. Nucl. Sci., 26 (1979) 2736.
28 R.R. Baris and A.L. Israel, Proc. Am. Acad. Cardiovasc. Perfus., 9 (1988) 37.
29 R.E. Davis, Lab. Pract., 15 (11) (1966) 1259.
30 R.H. Okada and H.P. Schwan, IRE Trans Biomed. Electron., 7 (1960) 188.
31 R. Firstenberg-Eden and G. Eden, Impedance Microbiology, Research Studies Press, Letchworth, 1984.
32 G.N. Stewart, J. Exp. Med., 4 (1899) 235.
33 E.H. Grant, R.J. Sheppard and G.P. South, Dielectric Behaviour of Biological Molecules in Solution, Clarendon Press, Oxford, 1978.
34 H.P. Schwan, in W.L. Nastuk (Ed.), Physical Techniques in Biological Research, Vol. VIB, Academic Press, New York, 1963, p. 323.
35 H.P. Schwan, Ann. N.Y. Acad. Sci., 148 (1968) 191.
36 D.B. Kell, in A.P.F. Turner, I.S. Karube and G.S. Wilson (Eds.), Biosensors: Fundamentals and Applications, Oxford University Press, Oxford, 1987 pp. 427–468.
37 C.L. Davey and D.B. Kell, in R. Paris (Ed.), Electric Field Phenomena in Biological Systems, IOP Short Meeting Series, IOP Bristol, 1989, pp. 51–62.
38 K.R. Foster and H.P. Schwan, Dielectric properties of tissues, in C. Polk and E. Postow (Eds.), CRC Handbook of Biological Effects of Electromagnetic Fields, CRC Press, Boca Raton, FL, 1986, pp. 27–96.
39 O.F. Schanne and E.R.P. Ceretti, Impedance Measurements in Biological Cells, Wiley, New York, 1978.
40 C.W. Einolf, Jr, and E.L. Carstensen, J. Phys. Chem., 75 (1971) 1091.
41 C.W. Einolf, Jr, and E.L. Carstensen, Biophys. J., 13 (1973) 8.
42 G. Schwarz, J. Phys. Chem., 66 (1962) 2636.
43 K. Asami, T. Hanai and N. Koizumi, J. Membr. Biol., 34 (1977) 145.
44 Y. Sugiura, S. Koga and H. Akabori, J. Gen. Appl. Microbiol., 10 (1964) 163.
45 C.M. Harris and D.B. Kell, Bioelectrochem. Bioenerg., 15 (1983) 415.
46 K. Asami, T. Hanai and N. Koizumi, J. Membr. Biol., 28 (1976) 169.

47 K. Asami, Bull. Inst. Chem. Res., Kyoto Univ., 55 (1977) 394.
48 A. Irimajiri, Y. Doida, T. Hanai and A. Hanai, J. Membr. Biol., 38 (1978) 209.
49 C.L. Davey, D.B. Kell, R.B. Kemp and R.W.J. Meredith, Bioelectrochem. Bioenerg., 20 (1988) 83.
50 A. Surowiec, S. Stuchly and C. Izaguirre, Phys. Med. Biol., 31 (1986) 43.
51 A. Irimajiri, K. Asami, T. Ichinowatari and Y. Kinoshita, Biochim. Biophys. Acta, 896 (1987) 203.
52 H.P. Schwan, Blut, 46 (1983) 185.
53 C.M. Harris and D.B. Kell, Eur. Biophys. J., 13 (1985) 11.
54 K. Asami, T. Hanai and N. Koizumi, Jpn. J. Appl. Phys., 19 (1980) 359.
55 L.E. Ferris, C.L. Davey and D.B. Kell, Eur. Biophys. J., 18 (1990) 267.
56 H. Fricke, Phys. Rev., 26 (1925) 678.
57 H. Fricke, J. Appl. Phys., 24 (1953) 644.
58 D.A.G. Bruggeman, Ann. Phys., 24 (1935) 636.
59 H. Fricke, Phys. Rev., 24 (1924) 575.
60 H. Fricke and S. Morse, Phys. Rev., 25 (1925) 361.
61 R.E. Meredith and C.W. Tobias, in C.W. Tobias (Ed.), Advances in Electrochemistry and Electrochemical Engineering, Wiley, New York, 1962, pp. 15–47.
62 A. Irimajiri, T. Hanai and A. Inouye, Experientia, 31 (1975) 1373.
63 R.W. Lovitt, R.P. Walter, J.G. Morris and D.B. Kell, Appl. Microbiol. Biotechnol., 23 (1986) 168.
64 G.H. Markx, C.L. Davey, D.B. Kell and P. Morris, J. Biotechnol., 20 (1991) 279.
65 C.M. Harris, R.W. Todd, S.J. Bungard, R.W. Lovitt, J.G. Morris and D.B. Kell, Enzym. Micr. Technol., 9 (1987) 181.
66 N.G. Stoicheva, C.L. Davey, G.H. Markx and D.B. Kell, Biocatalysis, 2 (1989) 245.
67 C.L. Davey, G.H. Markx and D.B. Kell, Eur. Biophys. J., 18 (1990) 255.
68 K.S. Cole and R.H. Cole, J. Chem. Phys., 9 (1941) 341.
69 G.H. Markx, C.L. Davey and D.B. Kell, Bioelectrochem. Bioenerg., 25 (1991) 195.
70 P.R. Bevington, Data Reduction and Error Analysis for the Physical Sciences, McGraw-Hill, New York, 1969, pp. 204–246.
71 J.R. Macdonald, J. Schoonman and A.P. Lehnen, J. Electroanal. Chem., 131 (1982) 77.
72 W.H. Press, B.P. Flannery, S.A. Teukolsky and W.T. Vetterling, Numerical Recipes: The Art of Scientific Computing (FORTRAN Version), Cambridge University Press, Cambridge, 1990, pp. 498–546.
73 R.J. Sheppard, J. Phys. D, 6 (1973) 790.
74 R.J. Sheppard, B.P. Jordan and E.H. Grant, J. Phys. D, 3 (1970) 1759.
75 R. Tamamushi and K. Takahashi, J. Electroanal. Chem., 50 (1974) 277.
76 G.H. Markx and D.B. Kell, Biofouling, 2 (1990) 211.
77 D.B. Kell, G.H. Markx, C.L. Davey and R.W. Todd, Trends Anal. Chem., 9 (1990) 190.
78 C.A. Boulton, P.S. Maryan and D. Loveridge, Proc. 22nd European Brewing Convention, Zürich, 1989, p. 653.
79 G.H. Markx, C.L. Davey and D.B. Kell, J. Gen. Microbiol., 137 (1991) 735.
80 J. Kronlöf, Eripainos Mallas ja Olut, 5 (1990) 140 (in Finnish).
81 G.H. Markx, H.J.G. ten Hoopen, J.J. Meijer and K.L. Vinke, J. Biotechnol., 19 (1991) 145.
82 G.J. Salter, D.B. Kell, L.A. Ash, J.M. Adams, A.J. Brown and R. James, Enzym. Micr. Technol., 12 (1990) 419.
83 C.L. Davey, W. Peñaloza, D.B. Kell and J.N. Hedger, World J. Microbiol. Biotechnol., 7 (1991) 248.
84 W. Peñaloza, C.L. Davey, J.N. Hedger and D.B. Kell, World J. Microbiol. Biotechnol., 7 (1991) 260.
85 H. Fricke, Nature, 172 (1953) 731.
86 A. Irimajiri, T. Hanai and A. Inouye, Biophys. Struct. Mechanism, 1 (1975) 273.
87 A. Irimajiri, K. Asami, T. Ichinowatari and Y. Kinoshita, Biochim. Biophys. Acta, 896 (1987) 203.
88 W. Jaroszynski, J. Terlecki and J. Sulocki, Studia Biophys., 107 (1985) 117.
89 T. Hanai, K. Asami and N. Koizumi, Bull. Inst. Chem. Res., Kyoto Univ., 57 (1979) 297.

90 H.P. Schwan and H.J. Morowitz, Biophys. J., 2 (1962) 395.
91 H.P. Schwan, S. Takashima, V.K. Miyamoto and W. Stoeckenius, Biophys., J., 10 (1970) 1102.
92 A.M. Woodward and D.B. Kell, Bioelectrochem. Bioenerg., 24 (1990) 83.
93 C.L. Davey and G.H. Markx, Binary, 14 (1988) 17.
94 D.W. Marquardt, J. Soc. Ind. Appl. Math., 11 (1963) 431.
95 F. Mosteller and J.W. Tukey, Data Analysis and Regression, Addison-Wesley, Reading, MA, 1977.
96 R.G. Duggleby, Anal. Biochem., 110 (1981) 9.
97 P. Gerhardt, R.G.E. Murray, R.N. Costilow, E.W. Nester, W.A. Wood, N.R. Krieg and G.B. Phillips, Manual of Methods for General Bacteriology, American Society for Microbiology, Washington, DC, 1981, pp. 182–183.
98 D.B. Kell, H.M. Ryder, A.S. Kaprelyants and H.V. Westerhoff, Antonie van Leeuwenhoek J. Microbiol. Serol., 60 (1991) 145.
99 K.P. Norris and E.O. Powell, J.R. Microscop. Soc., 80 (1961) 107.
100 T.B. Magath, J. Berkson and M. Horn, Am. J. Clin. Pathol., 6 (1936) 568.
101 J. Berkson, T. Magath and M. Horn, Am. J. Physiol., 128 (1940) 309.
102 F.G. Hirsch, E.C. Texter, L.A. Wood, W.C. Ballard, F.C. Horan and I.S. Wright, Blood, 5 (1950) 1017.
103 D.B. Kell, S.J. Ferguson and P. John, Biochim. Biophys. Acta, 502 (1978) 111.
104 D.B. Kell and C.M. Harris, Eur. Biophys. J., 12 (1985) 181.
105 K.S. Cole, Membranes, Ions and Impulses, University of California Press, Berkeley, CA, 1972.